



### Research Article

## Determination of the effect of artificial aging parameters on dry sliding wear resistance of 6013 aluminum alloy (Al-Mg-Si-Cu)

Mehmet Ayvaz<sup>a,\*</sup> 

<sup>a</sup>Vocational School of Manisa Technical Sciences, Manisa Celal Bayar University, Manisa 45140, Turkey

#### ARTICLE INFO

##### Article history:

Received 11 December 2020

Revised 12 February 2021

Accepted 05 March 2021

##### Keywords:

Aluminum

AA 6013

Artificial aging

Pin-on-disc

Dry sliding

#### ABSTRACT

In this study, the effect of artificial aging parameters, applied to AA6013 aluminum alloys commonly used in the automotive and aerospace sectors, on wear resistance was examined. For this purpose, AA6013 aluminum alloy samples were solutionized at 575 °C for 60 minutes and then they were artificially aged for 2, 4, and 6 hours at 180 and 200 °C temperatures. Mean hardness was measured as 66.6 HV in the solutionized samples taken. It was determined that as a result of artificial aging,  $\alpha$ -AlFeMnSi intermetallic phase precipitation were formed between  $\alpha$ -Al grains. By the effect of precipitation hardening, an increase in hardness was observed in all artificially aged samples; the highest hardness was found as an average of 149.3 HV in AA6013 samples aged artificially for 2 hours at 200 °C. A general decrease in the friction coefficients of samples aged at both 180 °C and 200 °C was observed along with the artificial aging temperature. The lowest specific wear rate was determined as  $3.542 \times 10^{-3} \text{ mm}^3/\text{Nm}$  in the AA6013 sample aged artificially for 2 hours at 200 °C.

© 2021, Advanced Researches and Engineering Journal (IAREJ) and the Author(s).

### 1. Introduction

Compared to steel and its alloys, aluminum and its alloys have been used in the automotive industry and in the aerospace industry since 1910 due to their high specific strength, corrosion resistance, and easy workability [1, 2]. Furthermore, the mechanical, physical, and chemical properties of heat-treatable 2XXX (Al-Cu), 6XXX (Al-Mg-Si) and 7XXX (Al-Zn-Mg) aluminum alloys can be improved by artificial aging. This precipitation hardening in aluminum alloys was coincidentally detected by Wilm in 1906 [3]. This phenomenon was also explained by Guinier and Preston independently of each other in 1938 [4, 5].

In 6XXX series Al-Mg-Si aluminum alloys, at the early stages of artificial aging, Mg and Si begin to precipitate from super-saturated solid solution (SSSS) formed with the solutionizing annealing, and then Guinier–Preston GP zones occur. In later stages, needle-like  $\beta''$  ( $\text{Mg}_5\text{Si}_6$ ) and rodlike  $\beta'$  phases are formed, respectively. As a result of long-term heat treatment, these metastable phases turn into stable  $\beta$ -

$\text{Mg}_2\text{Si}+\text{Si}$  phases [6, 7].

The 6013 aluminum alloy, a Cu-added Al-Mg-Si-Cu alloy of the 6XXX series, was first produced in the 1970s for the automotive sector with the aim of improving fuel efficiency. In later years, as a result of tests carried out at Lockheed and Alcoa Laboratories, the 6013 aluminum alloy was found to provide higher corrosion resistance despite having almost similar mechanical properties to the 2024 aluminum alloy used in aircraft, and it has begun to be used by Lockheed as structural aircraft material [8]. During aging in the Al-Mg-Si-Cu aluminum alloy, the needle-like  $\beta''$  phase transforms into the rodlike  $\beta^+$  lathlike  $\text{Q}'\text{-Al}_5\text{Cu}_2\text{Mg}_8\text{Si}_6$  phases. In the final stage, these phases also turn into  $\text{Q}+\beta\text{-Mg}_2\text{Si}+\theta\text{-Al}_2\text{Cu}+\text{Si}$  precipitate phases [9-11]. In addition, higher strengths are obtained by providing a smaller and finer distribution of precipitates formed by the addition of copper. This is because copper additions lead to smaller and finer dispersed precipitates [9].

Erdogan et al. applied artificial aging to 6013 aluminum alloy samples, which were solutionized at 530 °C, in a

\* Corresponding author. Tel.: +90 232 260 1001; Fax: +90 232 260 1004.

E-mail addresses: [m.ayvaz@cbu.edu.tr](mailto:m.ayvaz@cbu.edu.tr), [author.m.ayvaz@gmail.com](mailto:author.m.ayvaz@gmail.com) (M. Ayvaz)

ORCID: 0000-0002-9671-8679 (M. Ayvaz)

DOI: 10.35860/iarej.839108

This article is licensed under the CC BY-NC 4.0 International License (<https://creativecommons.org/licenses/by-nc/4.0/>).

microwave oven for 3 different periods of 1, 3, and 5 hours at 190 °C. The highest hardness values were obtained in samples aged artificially for 3 hours around 70 HV, and the highest corrosion resistance was also obtained in these samples. It was reported that FeAl intermetallic phases improved both mechanical properties and corrosion resistance. [12].

After taking 5068, 6061, and 6013 aluminum alloys into the solution at 530 °C, Zeid artificially aged them for 30 minutes at 175 °C and then compared their mechanical properties and corrosion resistance. In the study, Mg<sub>2</sub>Si with orientation (420), (422) and (511) was detected in natural and artificially aged AA 6013 alloy. After the aging heat treatment, the highest hardness values were obtained in 6013 aluminum alloy. In addition, 6013 and 6061 aluminum alloys exhibited higher corrosion resistance than 5086 [13].

In their study, Liu et al. took 6013 aluminum alloy samples into the solution at 560 °C for 2 hours, then artificially aged them at 191°C and different periods between 10 min-24 h, and examined their mechanical properties. The highest hardness value was measured as approximately 111 HV in the sample aged for 4 h. They also found the highest yield and tensile strength in this sample to be 258 and 310 MPa, respectively [14].

After taking 6013 aluminum alloys into the solution at 560 °C for 8 hours, Akyüz and Şenaysoy aged them artificially at 180°C for 1,3, 6, 9, 12, and 24 hours. 6 hours of artificial aging revealed optimum values in terms of time and mechanical properties. As a result of machinability experiments, they determined that the shear force increased with aging time [15]. In another study conducted with the same aging heat treatment parameters, they examined the mechanical and machinability properties of 6013 and 6082 aluminum alloys comparatively. In tests carried out with a shear rate of 60 m·min<sup>-1</sup>, as a result of aging, lower shear forces were measured and higher surface quality was obtained in 6013 aluminum alloy with higher mechanical properties compared to 6082 aluminum alloy [16].

One of the limits of use of aluminum alloys is low wear resistance. In many studies in the literature, the mechanical properties, machinability, and corrosion resistance of the 6013 aluminum alloy after artificial aging heat treatment have been examined and optimal heat treatment parameters have been identified. However, the effect of artificial aging on the tribological properties and wear resistance of the 6013 aluminum alloy have not been revealed and optimal parameters have not been determined. In this study, the relationship between aging heat treatment and wear resistance was revealed.

## 2. Materials and Method

First, 6013 aluminum alloy samples were cut in a way that they would be Ø30 mm and 10 mm thickness. The lower and upper surfaces of the cut samples were sanded with 180-1200

grit sandpapers. The prepared samples were solutionized for 60 minutes at 575 °C in the Protherm brand Ash furnace and then cooled in the water at room temperature. Artificial aging heat treatment was applied for 2, 4, and 6 hours at temperatures of 180 °C to one part of the samples were solutionized and at 200 °C to the other part of the samples. Spectral analysis of the used AA6013 aluminum alloy samples is given in Table 1.

Micro-hardness measurements of the samples solutionized and aged were performed with the Vickers hardness tester (Future-Tech Corp FM-700, Tokyo, Japan). In these tests, which were implemented in accordance with ASTM E384–17 standards, measurements were repeated at least 5 times for each sample with a sinking time of 10 seconds under a 50gf load. The wear test surfaces of the samples were polished with 3 and 1 µm diamond polishers. Then, wear tests of these samples were then carried out on the CSM Tribometer model wear tester (Anton Paar, Switzerland) in accordance with ASTM G99–17 standard. Tests were conducted with dry sliding, under 10 N Load, with a sliding speed of 20 cm·sec<sup>-1</sup>. 100Cr6 balls with a diameter of 6 mm were used as counter elements in the tests (Figure 1).

For metallographic examinations, 6013 aluminum alloy samples, whose surfaces were sanded and polished, were etched with Keller solution (2.5 ml HNO<sub>3</sub>, 1.5 ml HCl, 1 ml HF, 95 ml water). Microstructure and wear surface examinations of the samples were carried out with the ZEISS GeminiSEM 500 FE-SEM model (ZEISS, Oberkochen, Germany) scanning electron microscope (SEM).

Table 1. Chemical composition (wt.%) of AA6013 aluminum alloy samples

Element	Wt %
Al	95.96
Si	0.903
Cu	0.767
Mg	1.002
Mn	0.412
Fe	0.645
Zn	0.179
Cr	0.036
Other	0.096

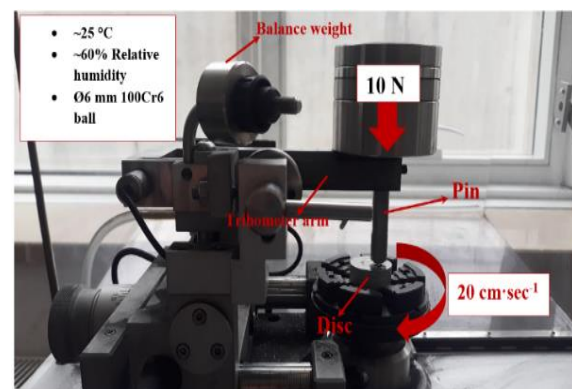


Figure 1. Pin-on-disc tribometer

### 3. Results and Discussion

Microhardness values of samples solutionized and artificially aged for 2, 4, and 6 hours at 180 and 200 °C are presented in Figure 2. The microhardness value of solutionized AA6013 aluminum alloy was determined as 66.6 HV on average. In samples aged artificially at 180 °C, as aging time increased, an increase in the microhardness values of AA6013 samples occurred; the microhardness values for these samples were measured on average as 89.8, 112.6, and 117.2, respectively. Hardness increase, occurring as a result of precipitation and precipitation hardening emerging due to artificial aging, is a well-known mechanism [10, 17-19]. The increase in hardness reaches the peak point at different artificial aging times, and at the end of aging time, a decrease occurs again. This case was clearly seen in the samples aged artificially at 200 °C. In AA6013 aluminum alloy samples that were aged artificially at 200 °C, microhardness values were measured as 149.3, 142.8, and 130.6 HV for aging times of 2, 4, and 6 hours, respectively. It is known that the T6 heat treatment of AA6013 is performed for 4 hours at 190 °C [20].

In this study, by heat treatment performed for 2 hours at 200 °C, peak artificial aging was achieved and a 2.2 times increase in microhardness was obtained in these samples compared to the solutionized samples.

In Figure 3a-f, SEM images of the microstructures of the samples aged artificially for 2, 4, and 6 hours at temperatures of 180 and 200 °C are shown. When the internal structures are examined, precipitate formations in the  $\alpha$ -Al matrix are seen in all samples. The SEM images of this precipitate was taken from sample of it aged artificially for 4 hours at 180 °C and an EDS analysis was performed (Figure 4). The precipitate formed by artificial aging had almost round

structure and was in sizes of 1-1.5  $\mu$ m. EDS analysis showed that this precipitate was an  $\alpha$ -AlFeMnSi intermetallic compound. In their study, Barbosa et al. determined that  $\alpha$ -AlFeMnSi precipitates of 800-900 nm in the round structure were formed as a result of artificial aging processes that were realized at different times at 180 °C [11]. They also reported that the Mn/Fe ratio in that precipitate was  $0.58 \pm 0.12$ . In this study too, this ratio was determined to be approximately 0.55.

In Figure 5, for post wear-tests, volume losses and specific wear rates of solutionized sample and samples aged artificially for 2, 4 and 6 hours at 180 and 200 °C are given. The specific wear rate of solutionized the sample was determined as  $\sim 6.12 \times 10^{-3}$  mm<sup>3</sup>/Nm. In samples artificially aged for 2 and 4 hours at 180 °C, whereas there was a decrease in specific wear rates, no significant wear resistance was observed. Specific wear rates for these samples were  $\sim 5.90 \times 10^{-3}$  and  $5.38 \times 10^{-3}$  mm<sup>3</sup>/Nm, respectively. With  $\sim 18\%$  reduction, the specific wear rate in the sample aged artificially for 6 hours at 180 °C became  $\sim 5.01 \times 10^{-3}$  mm<sup>3</sup>/Nm. By artificial aging heat treatment performed for 2 hours at 200 °C, the specific wear rate of the AA6013 aluminum alloy sample decreased by  $\sim 42\%$  and became  $\sim 3.54 \times 10^{-3}$  mm<sup>3</sup>/Nm. After aging treatments performed for 4 and 6 hours at this temperature, specific wear rates were determined as  $\sim 4.64 \times 10^{-3}$  and  $5.60 \times 10^{-3}$  mm<sup>3</sup>/Nm, respectively. Previous studies have generally reported that wear resistance of the aluminum alloy increases with peak aging and there is a relationship between hardness and wear resistance [21-23]. In 6XXX series aluminum alloys, Mg<sub>2</sub>Si, Al<sub>2</sub>Cu and AlFeSi precipitates formed with artificial aging play an important role in this increase in hardness and wear resistance [22, 24, 25].

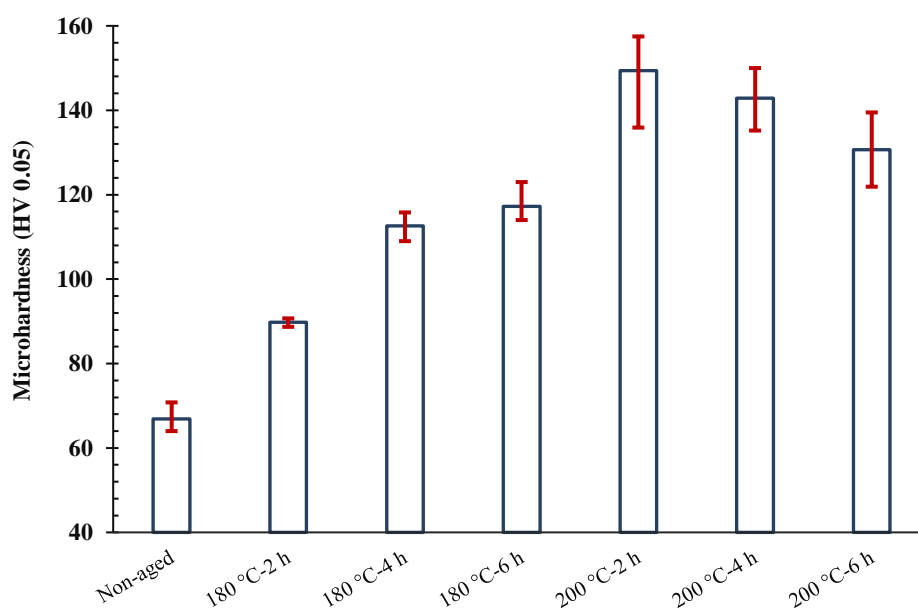


Figure 2. Microhardness of AA6013 samples solutionized and aged artificially

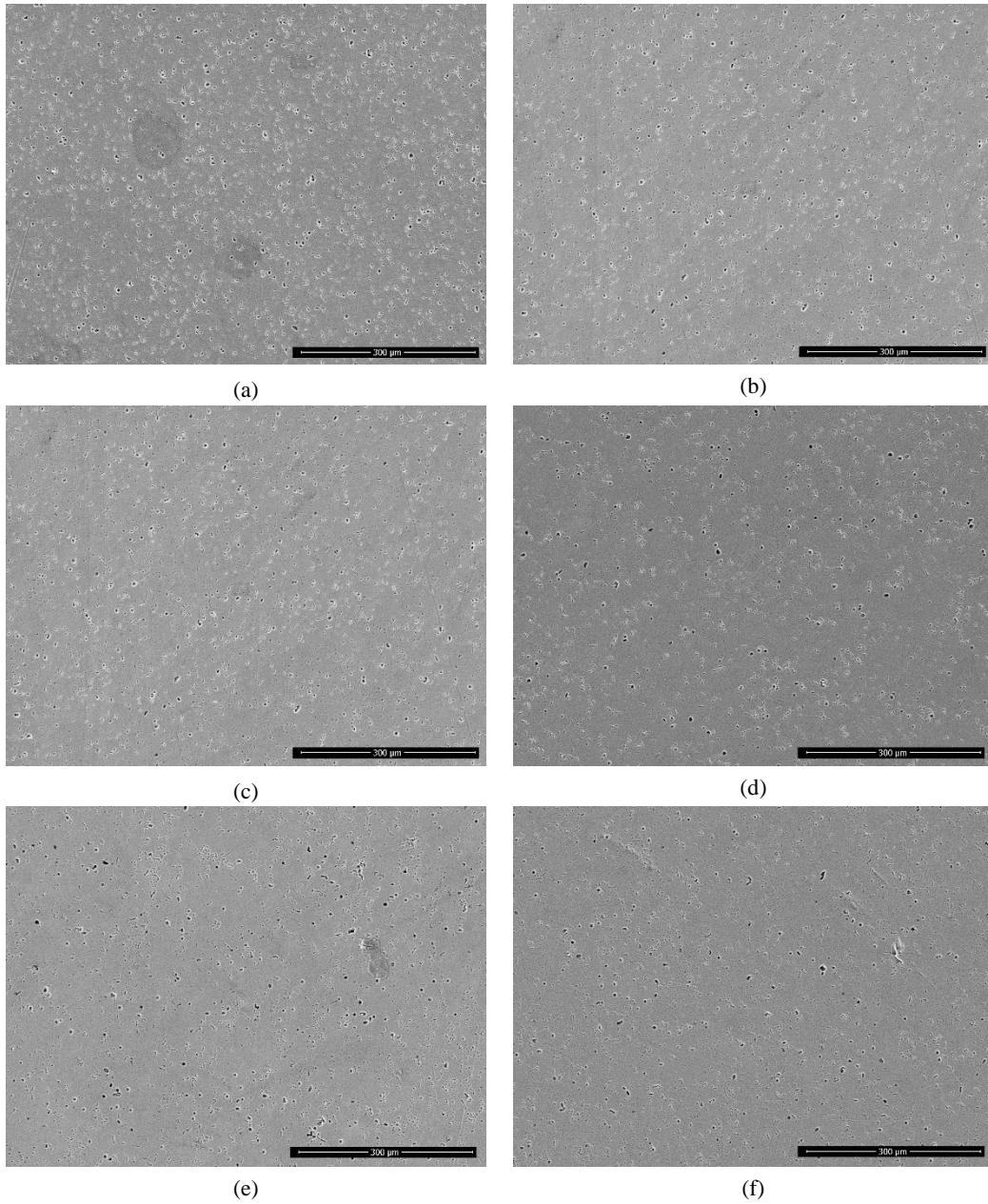


Figure 3. SEM images of internal structures of artificially aged samples: a) 180 °C-2h, b) 180 °C-4h, c) 180 °C-6h, d) 200 °C-2h, e) 200 °C-4h and f) 200 °C-6h.

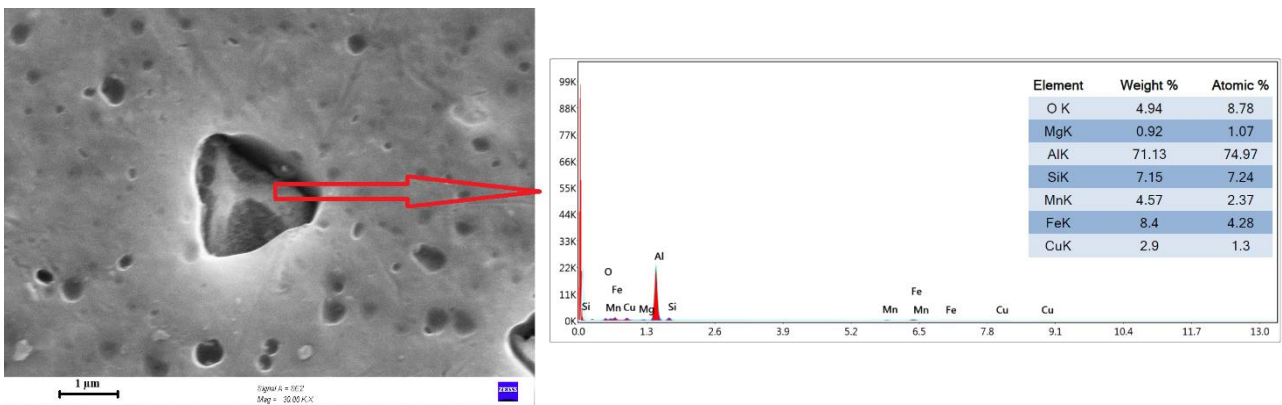


Figure 4. SEM image and EDS analysis of  $\alpha$ -AlFeMnSi precipitate in the sample aged artificially for 4 hours at 180 °C.

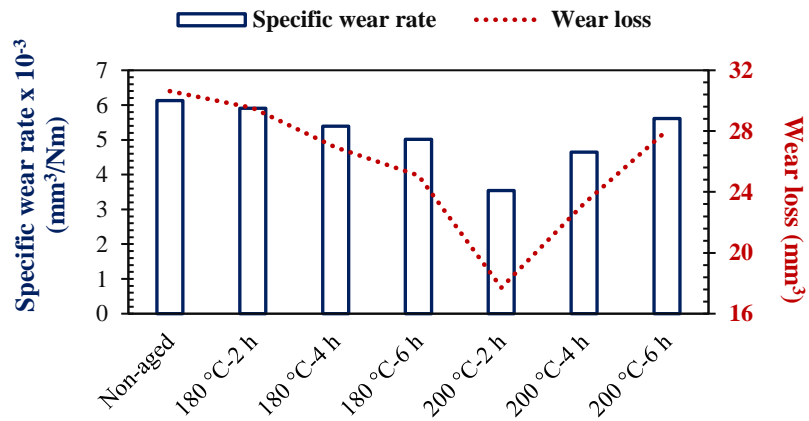


Figure 5. Wear losses and specific wear rates of solutionized and aged AA6013 aluminum alloy samples.

Figure 6 shows SEM images taken from the wear surfaces of AA6013 aluminum alloy samples that have been solutionized and aged. It can be seen in these SEM images

that in the solutionized sample and in the samples aged for 2, 4 and 6 hours at 180 °C after being solutionized, the dominant wear type is delamination wear (Figures 6a-d)

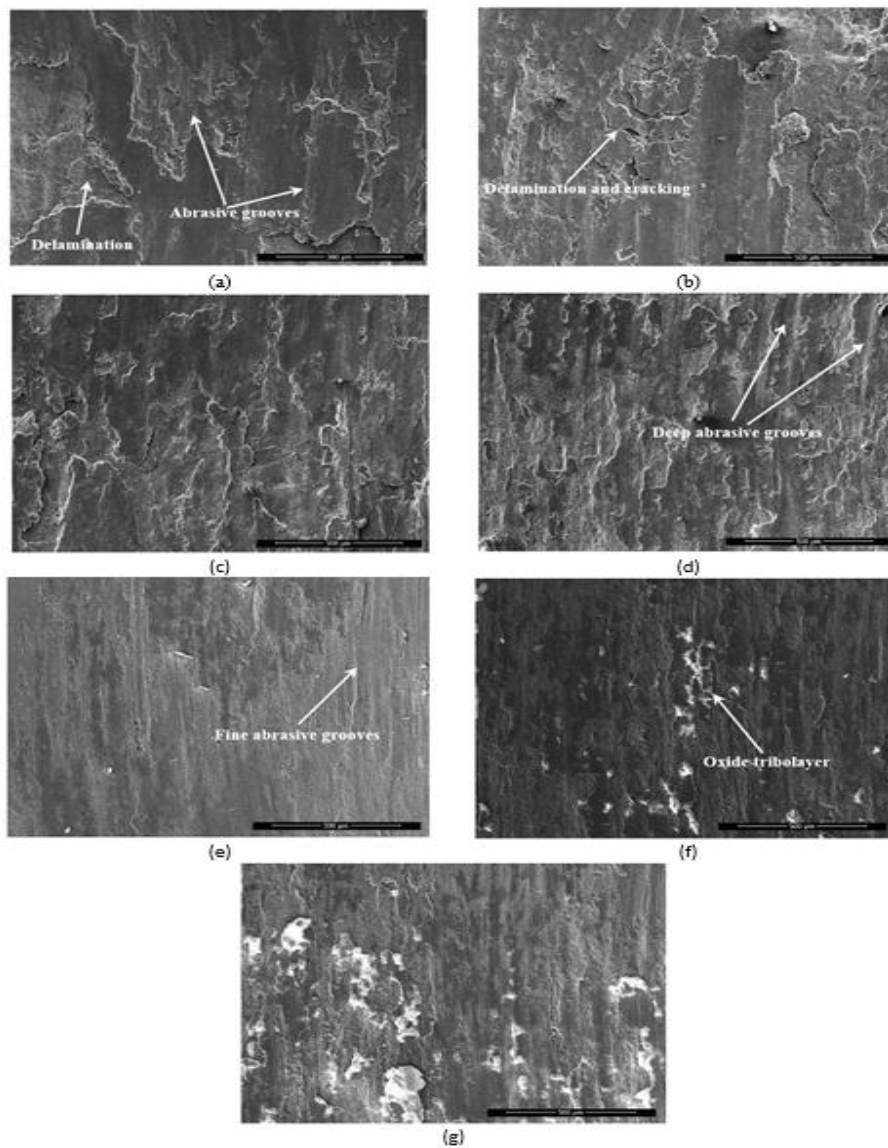


Figure 6. SEM images of wear surfaces of the heat treated AA6013 samples: a) solutionized, b) 180 °C-2h, c) 180 °C-4h, d) 180 °C-6h, e) 200 °C-2h, f) 200 °C-4h and g) 200 °C-6h.

Abrasive wear scratches in these samples also indicate the presence of abrasive wear. In the sample to which aging process has been applied at 200 °C for 2 hours, the width of the wear trace appears to be narrower compared to other samples (Figure 6e). In addition, delamination wear has almost never occurred in this sample. But traces of abrasive wear are also evident in this sample. Moreover, on the wearing surface, intense crack formation, which occurs as a result of plastic deformation resistance increasing with increased hardness, is observed. Plastic deformation and flow traces are again observed in samples aged for 4 and 6 hours at 200 °C (Figures 6f, g). In addition, oxidative wear traces and tribolayers were identified on the wear surfaces of these samples and this was also detected by EDS analysis results obtained from the surface of the sample, which was aged for 4 hours at 200 °C (Figure 7).

In Figure 8, sliding distance dependent friction coefficients of the samples aged for 2, 4, and 6 hours at 180 °C and 200 °C are given. The mean friction coefficient of the solutionized sample was determined as 0.502. In samples that underwent artificial aging heat treatment at 180 °C for 2 and 4 hours, the mean friction coefficients were also found to be 0.503 and 0.502, respectively. In the sample aged artificially for 6 hours, on the other hand, the mean friction coefficient decreased slightly and became 0.470. Similarly, in the samples aged artificially at 200 °C, the lowest mean coefficient of friction was measured as 0.440 in the sample aged artificially for 6 hours. Among all samples solutionized and aged artificially, the highest mean friction coefficient was determined in the sample aged artificially for 2 hours at 200 °C. In addition, when graphs of change in the sliding distance dependent friction coefficient were examined, it was seen that the running-in period decreased and the steady-state was reached in a shorter time with an increase in artificial aging temperature and time.

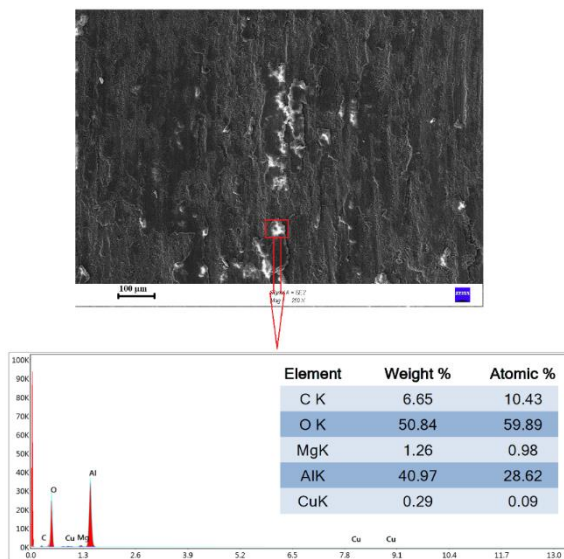


Figure 7. EDS analysis results obtained from the surface of the sample, which was aged for 4 hours at 200 °C

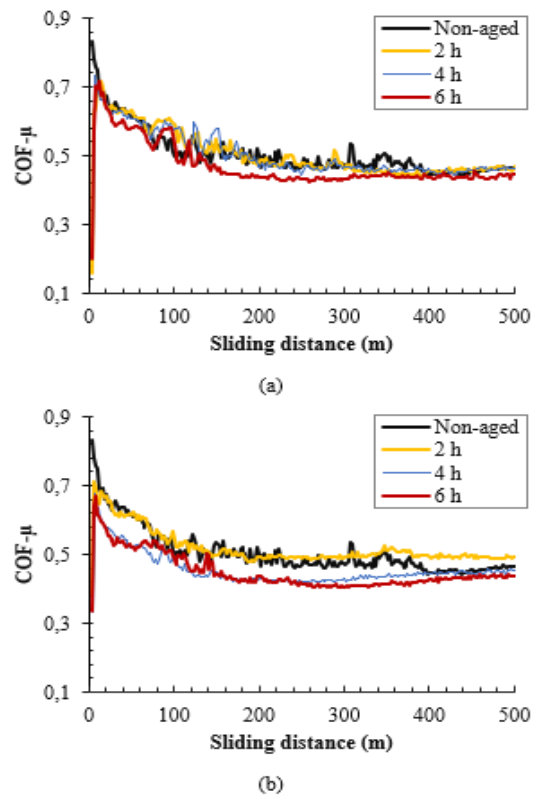


Figure 8. Sliding distance dependent friction coefficients of the artificial aged samples

#### 4. Conclusion

As a result of microstructural and tribological investigations of the non-aged and artificial aged AA6013 samples, the determined results are as follows:

- The hardness of the solutionized sample is 66 HV.
- Peak-aged samples are samples aged artificially for 2 hours at 200 °C. The hardness of these samples is 149.3 HV.
- By artificial aging,  $\alpha$ -AlFeMnSi precipitates that have a low Mn/Fe ratio, 1-1.5  $\mu\text{m}$  diameter, and almost round structure are formed.
- The sample that has the highest friction coefficient ( $\mu=0.517$ ) and the lowest specific wear rate ( $\sim 3.54 \times 10^{-3} \text{ mm}^3/\text{Nm}$ ) is the sample aged artificially for 2 hours at 200 °C.
- In AA6013 samples, while plastic deformations and delamination type wear are observed as hardness decreases, abrasive wear becomes dominant as hardness increases (against 60-65 HRc 100Cr6 ball counterpart).

#### Declaration

The author declared no potential conflicts of interest with respect to the research, authorship, and/or publication of this article. The author also declared that this article is original, was prepared in accordance with international publication and research ethics, and ethical committee permission or any special permission is not required.

## Author Contributions

M. Ayvaz is responsible for all section of the study.

## References

1. Atilio I., Braga, V., Siqueira, R. H. M., Carvalho, S. M., Lima, M. S. F., *Comparing the weldability of AA6013-t4 aluminium alloy on DP600 dual-phase steel with laser welding and resistance spot welding*, Journal of the Brazilian Society of Mechanical Sciences and Engineering, 2020. **42**(71): p. 1-12.
2. Şimşek, İ., Şimşek, D., Özyürek, D., *The effect of different sliding speeds on wear behavior of ZrO<sub>2</sub> reinforcement aluminium matrix composite materials*. Internatioal Advanced Researches and Engineering Journal, 2020. **4**(1): p. 1-7.
3. Wilm, A., *Physico-metallurgical investigations of aluminium alloys containing magnesium*. Metallurgie, 1911. **8**: p. 255-227.
4. Guinier, A., *Structure of age-hardened aluminium-copper alloys*. Nature, 1938. **14**: p. 569–570.
5. Preston, G. D., *The diffraction of x-rays by age-hardening aluminium copper alloys*. Proceedings of the Royal Society of London, 1938. **167**(931): p. 526-538.
6. Dutta, I., Allen, S.M., *A calorimetric of precipitation in commercial aluminum alloy 6061*. Journal of Materials Science Letters, 1991. **10**: p. 323-326.
7. Pogatscher, S., Antrekowitsch, H., Leitner, H., Ebner, T., Uggowitzer, P. J., *Mechanisms controlling the artificial aging of Al–Mg–Si alloys*. Acta Materialia, 2011. **59**: p. 3352-3363.
8. Kaneko, R.S., Bakow, L., Lee, E.W., *Aluminum alloy 6013 sheet for new U.S. navy aircraft*. JOM, 1990. **42**: p. 16-18.
9. Staab, T.E.M., Krause-Rehberg, R., Hornauer, U., Zschech, E., *Study of artificial aging in AlMgSi (6061) and AlMgSiCu (6013) alloys by Positron Annihilation*. Journal of Material Science, 2006. **41**: p. 1059–1066.
10. Buha, J., Lumley, R.N., Crosky, A.G., Hono, K., *Secondary precipitation in an Al–Mg–Si–Cu alloy*. Acta Materialia, 2007. **55**: p. 3015-3024.
11. Barbosa, C., Rebello, J.M.A., Acselrad, O., Dille, J., Delplancke, J.-L., *Identification of precipitates in 6013 aluminum alloy (Al–Mg–Si–Cu)*. International Journal of Materials Research, 2002. **93**(3): p. 208-211.
12. Erdoğan, M., Tekin, R., Kaya, M., *Mikrodalga fırında suni yaşlandırılan 6013 alüminyum alaşımın korozyon davranışının incelenmesi (Investigation of corrosion behavior of 6013 aluminum alloy aged artificially in microwave oven)*. Pamukkale Üniversitesi Mühendislik Bilimleri Dergisi, 2014. **20**(1): p. 25-30.
13. Abo Zeid, E.F., *Mechanical and electrochemical characteristics of solutionized AA 6061, AA6013 and AA 5086 aluminum alloys*. Journal of Materials Research and Technology, 2019. **8**(2): p. 1870-1877.
14. Liu, M., Jiang, T., Wang, J., Liu, Q., Wu, Z., Yu, Y., Skaret, P.C., Roven, H. J., *Aging behavior and mechanical properties of 6013 aluminum alloy processed by severe plastic deformation*. Transactions of Nonferrous Metals Society of China, 2014. **24**: p. 3858-3865.
15. Akyüz, B., Şenaysoy, S., *Effect of the aging process on mechanical properties and machinability in AA6013 aluminum alloys*. Scientific Research and Essays, 2015. **10**(2): p. 17-78.
16. Akyüz, B., Şenaysoy, S., *Effect of aging on mechanical properties and machining on aluminum alloys*. Bilecik Şeyh Edebali Üniversitesi Fen Bilimleri Dergisi, 2014. **1**(1): p. 1-9.
17. Cuniberiti, A., Tolley, A., Castro Riglos, M.V., Giovachini, R., *Influence of natural aging on the precipitation hardening of an AlMgSi alloy*. Materials Science and Engineering A, 2010. **527**: p. 5307-5311.
18. Esmaeili, S., Wang, X., Lloyd, D.J., Poole, W.J., *On the precipitation-hardening behavior of the Al–Mg–Si–Cu alloy AA6111*. Metallurgical and Materials Transactions A, 2003. **34**: p. 751-763.
19. Murayama, M., Hono, K., *Pre-precipitate clusters and precipitation processes in Al–Mg–Si alloys*. Acta Materialia, 1999. **47**(5): p. 1537-1548.
20. Heat Treating, ASM Handbook, Volume 4 (1991): *Heat Treating of Aluminum Alloys*.
21. Das, S., Pelcastre, L., Hardell, J., Prakash, B., *Effect of static and dynamic ageing on wear and friction behavior of aluminum 6082 alloy*. Tribology International, 2013. **60**: p. 1-9.
22. Meyveci, A., Karacan, İ., Çalığülü, U., Durmuş, H., *Pin-on-disc characterization of 2xxx and 6xxx aluminum alloys aged by precipitation age hardening*. Journal of Alloys and Compounds, 2010. **491**: p. 278-283.
23. Baydoğan, M., Çimenoglu, H., Kayali E.S., *A study on sliding wear of a 7075 aluminum alloy*. Wear, 2004. **257**: p. 852-861.
24. Gavgali, M., Totik, Y., Sadeler, R., *The effects of artificial aging on wear properties of AA 6063 alloy*. Materials Letters, 2003. **57**: p. 3713-3721.
25. Meriç, C., Atik, E., Kaçar, H., *Effect of aging on abrasive wear of deformable aluminum alloy AA6351*. Metal Science and Heat Treatment, 2004. **46**(3-4): p. 110-114.